Theor Chim Acta (1989) 75: 11-32

Theoretica Chimica Acta

The classification of tensor surface harmonic functions for clusters and coordination compounds

Roy L. Johnston and D. Michael P. Mingos

Inorganic Chemistry Laboratory, University of Oxford, South Parks Road, Oxford OX1 3QR, UK

(Received August 27, 1987; revised April 22 and May 24/Accepted May 25, 1988)

A simple method for enumerating the L^{σ} and $L^{\pi}/\bar{L}^{\pi}$ functions for polyhedral cluster and coordination molecules, within Stone's tensor surface harmonic methodology, is described. The nature of the L^{σ} orbitals which are generated depends on the polyhedral topology and in particular the number of layers of vertices and the number of vertices within each layer. The $L^{\pi}/\bar{L}^{\pi}$ functions are enumerated from the L^{σ}'s by a number of spherical harmonic multiplication rules.

Key words: Tensor surface harmonics — Clusters — Polyhedral topology — Classification

1. Introduction

According to Stone's tensor surface harmonic (TSH) theory [1-4], the vertices of a cluster molecule are defined as lying on the surface of a single sphere, with each atom (i) assigned the angular coordinates (θ_i, ϕ_i), as shown in Fig. 1. The solutions of the Schrödinger equation for a particle on a sphere are based on spherical harmonic functions which may, as in the case of atomic orbitals, be assigned L and M quantum numbers [5]. The cluster MO's $(\Psi_{L,M})$ are generated from the general spherical harmonics $S_{L,M}(\theta, \phi)$ according to the following LCAO expansion based on atomic or hybrid orbitals (ρ_i) [1, 2]:

$$\Psi_{L,M} = N \Sigma_i c_i \rho_i = N \Sigma_i S_{L,M}(\theta_i, \phi_i) \rho_i$$

The spherical harmonics $S_{L,M}$ can be scalar spherical harmonics $(Y_{L,M})$ if the atomic orbitals are nodeless (i.e. σ-type) with respect to the radial vector, vector surface harmonics if the atomic orbitals are singly noded (i.e. π-type) or tensor

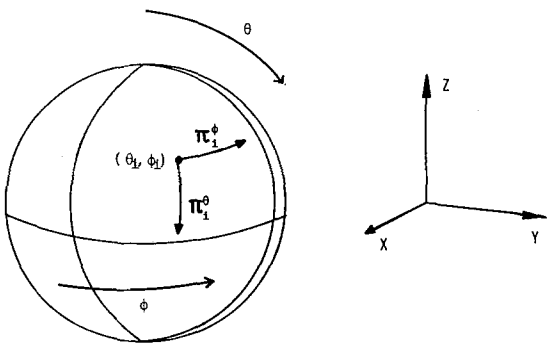

Fig. 1. The angular coordinate system used in tensor surface harmonic theory

surface harmonics if they are doubly noded (i.e. δ-type). Two vector or tensor surface harmonic functions can be generated from each $Y_{L,M}$, as follows [1, 2]:

(*i*) *Vector surface harmonics*

$\boldsymbol{V}_{L,M} = \nabla Y_{L,M}$ (i.e. the gradient of $Y_{L,M}$, $\nabla = (\partial/\partial\theta) + (\sin\theta)^{-1}(\partial/\partial\phi)$).

$\bar{\boldsymbol{V}}_{L,M} = \boldsymbol{r} \times \nabla Y_{L,M}$ (the *parity inverse* of $\boldsymbol{V}_{L,M}$, corresponding to a rotation of each atomic π-function by 90° about the radial vector $\boldsymbol{r}$ [1–3]).

(*ii*) *Tensor surface harmonics*

$\boldsymbol{T}_{L,M} = \nabla\nabla Y_{L,M}$ (i.e. the concavity of $Y_{L,M}$).

$\bar{\boldsymbol{T}}_{L,M} = \boldsymbol{r} \times \nabla\nabla Y_{L,M}$ (the parity inverse of $\boldsymbol{T}_{L,M}$, corresponding to rotation of each atomic δ-function by 45° about the radial vector [1–3]).

The resulting cluster wavefunctions are denoted as follows: $\Psi^\sigma_{L,M} (\equiv L^\sigma_M; L = 0(S), 1(P), 2(D)$ etc.); $\Psi^\pi_{L,M}/\bar{\Psi}^\pi_{L,M} (\equiv L^\pi_M/\bar{L}^\pi_M; L = 1, 2, 3$ etc.); $\Psi^\delta_{L,M}/\bar{\Psi}^\delta_{L,M} (\equiv L^\delta_M/\bar{L}^\delta_M; L = 2, 3, 4$ etc.).

For main group clusters, the cluster vertex atoms possess σ- and π-type frontier orbitals only. Thus, cluster bonding may be described in terms of L^σ, L^π and $\bar{L}^\pi$ functions. In this way, Stone has used TSH theory to derive the $(n+1)$ skeletal electron pair (SEP) rule [6] for *closo* deltahedral boranes $[B_nH_n]^{2-}$ [1, 2] and their $(n-1)$-vertex *nido* and $(n-2)$-vertex *arachno* derivatives [3]. The methodology has been extended to 3-connected hydrocarbon clusters $[C_nH_n]$ [7], 4-connected clusters [8] and bispherical clusters (i.e. those where the cluster vertices lie on the surfaces of two spheres of differing radii [9]).

Quinn et al. have developed an elegant group theoretical methodology whereby the symmetries of the L^σ, $L^\pi/\bar{L}^\pi$ and $L^\delta/\bar{L}^\delta$ orbitals may be evaluated using a number of simple multiplication rules [10–13]. The combination of group theory and TSH theory has been utilised by Fowler [14, 15] and ourselves [16–18] to rationalise the pattern of skeletal MO's in a number of cluster molecules and, in particular, to account for deviations from the $(n+1)$ SEP rule in a number of topologically distinct classes of deltahedral clusters [14, 16, 17].

The TSH methodology is also appropriate for the generation of linear combinations of ligand orbitals in cluster and coordination compounds [1, 10]. The

complementary spherical electron density (CSED) model accounts for the inert gas rule and the stereochemistries of main group and transition metal molecules [19-21]. The cluster and ligand-sphere applications of TSH theory have been combined in a study of face- and edge-bridged octahedral clusters of the form $[M_6(\mu_3-X)_8X_6]$ and $[M_6(\mu-X)_{12}X_6]$, where X is either a π-acceptor ligand (e.g. CO) or a π-donor ligand (e.g. Cl) [22].

In all of the above mentioned applications of TSH theory, the ligand or cluster linear combinations were derived explicitly by evaluating the values of the spherical harmonic functions for all (θ_i, ϕ_i) atomic coordinates. In this paper, relationships between the topologies of the (ligand or cluster) polyhedra and the adoption of specific spherical harmonic functions are developed. These generalisations greatly assist qualitative applications of tensor surface harmonic theory. This approach is entirely complementary to the group theoretical methodology of Quinn et al. and should be used in conjunction with these symmetry-based arguments to obtain a full (symmetry and spherical harmonic) definition of the L^σ and $L^\pi/\bar{L}^\pi$ orbitals. Useful tables of the symmetry transformation properties of σ-, π- and δ-type functions for a large number of polyhedral geometries, have been derived by Fowler and Quinn [13].

2. Null and redundant spherical harmonic functions

Although the TSH and CSED models use solutions of the particle on a sphere problem, the atoms define a specific polyhedron belonging to a finite point group and, consequently, some of the spherical harmonic functions are either zero-valued at all vertex positions (*null functions*) or generate linear combinations which are repetitions of previously used lower order spherical harmonics (*redundant functions*). The *null functions* result from the location of polyhedral vertices on nodal planes of the spherical harmonic functions and therefore occur as a consequence of general topological features of the polyhedron. The *redundant functions* result because the finite arrangement of atoms merely constitute a subset of the infinite number of points which define the sphere, and this limited subset has a specific maximum number of nodal planes which determines whether or not spherical harmonic functions with differing L and M quantum numbers are distinguishable.

For rings and prisms, where all of the vertices are equivalent (i.e. they are "single orbit" structures [13]) and consist of n-membered rings which are perpendicular to the principal rotation axis, C_n, the null L^σ functions are particularly simple. For a ring, those functions $L^\sigma_{\pm M}$ (where $L+M$ is odd) are null functions, since they are noded in the equatorial plane on which the ring lies. When n is even, the function $\mathscr{L}^\sigma_{\mathscr{L}s}$, where $\mathscr{L}=n/2$, is also a null function, for both rings and prisms (in this analysis, all polyhedra are defined such that the first vertex of the first layer is situated at $\phi=0°$).

The redundant L^σ functions for rings, prisms and antiprisms (or $2n$-vertex puckered rings) are listed in the Appendix. Subtraction of the null and redundant

functions from the complete set of spherical harmonics leaves us with the L^σ functions utilised by rings, prisms and antiprisms (see Tables 1, 3 and 5).

3. Rings

3.1. L^σ functions

For (planar) rings with even numbers of atoms (n) the L^σ functions generated are listed in Table 1.

The adopted L^σ functions can also be expressed in terms of the solution of the Schrödinger Equation for a particle on a ring, i.e. only one quantum number is required since $M = L$ [23]. The ring cluster functions are quantised with respect to a single rotation axis and the only possible nodal planes (which do not lead to null functions) are those ("vertical") nodal planes which are parallel to (and contain) this axis.

3.2. Generation of π-functions by multiplication of TS harmonics

Quinn has shown that the tangential π-type functions of a polyhedron can be generated by taking the L^σ functions and replacing the atomic σ-orbitals by tangential (p^π) orbitals whose relative signs (i.e. the directions of the vectors) are given by the phases of the π-functions [10–12]. The p^π orbitals are taken to lie along lines of increasing $\theta(\pi^\theta)$ or ϕ (π^ϕ), as shown in Fig. 1. Quinn demonstrated that this superposition technique (which is similar in nature to the generator orbital method of Verkade et al. [24, 25]) corresponds to the following Group Theoretical multiplication rules [10–18]:

$\Gamma^\theta_{\pi+\bar{\pi}} = \Gamma_\sigma \times \Gamma_z$ since the θ coordinate transforms as the polar vector z.

$\Gamma^\phi_{\pi+\bar{\pi}} = \Gamma_\sigma \times \Gamma_{R_z}$ since the ϕ coordinate transforms as the axial pseudo-vector R_z.

Utilising the notation of tensor surface harmonic theory, the following analogous multiplication rules can be proposed:

Table 1. L^σ functions generated for planar n-gonal rings

n								
3	S^σ_0	$P^\sigma_{\pm1}$						
4	S^σ_0	$P^\sigma_{\pm1}$	D^σ_{2c}					
5	···	···	$D^\sigma_{\pm2}$					
6	···	···	···	F^σ_{3c}				
7	···	···	···	$F^\sigma_{\pm3}$				
Even n	···	···	···	···	$L^\sigma_{\pm L}$	···	$\mathscr{L}^\sigma_{\mathscr{L}c}$	$\mathscr{L} = n/2$
Odd n	···	···	···	···	$L^\sigma_{\pm L}$	···	$\mathscr{L}^\sigma_{\pm\mathscr{L}}$	$\mathscr{L} = (n-1)/2$

$\{L^\pi/\bar{L}^\pi\}^\theta = L^\sigma \times P_0^\pi$ (P_0^π is the vector surface harmonic function with polar (z) character (*1*).

$\{L^\pi/\bar{L}^\pi\}^\phi = L^\sigma \times \bar{P}_0^\pi$ (P_0 is the vector surface harmonic function with axial (R_z) character (*2*).

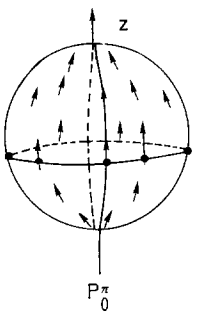

(*1*)

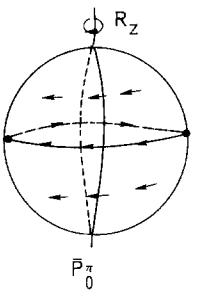

(*2*)

The θ and ϕ components of the tangential orbital set are related by the parity inversion operator ($\mathscr{P}$) [1-3], since P_0^π and $\bar{P}_0^\pi$ are so related.

Using the above methodology, the L^π and $\bar{L}^\pi$ functions for a planar ring are obtained from the L^σ functions by a superposition of the atomic π-orbitals on the L^σ functions. The effect of multiplying L_M^σ by P_0^π is to increase the L quantum number by 1, while leaving M unchanged. This follows by analogy with the modified Clebsch-Gordan formula for axial point groups [26]:

$$D_M^L \times D_0^1 = D_M^{L+1}$$

(where $D^0 = S$, $D^1 = P$ etc.).

Since the rings are defined as lying in the equatorial plane, there is no mixing between the θ and ϕ components of the tangential orbitals. Therefore the multiplication rules (or $\sigma - \pi$ mapping) may be stated:

$$L_{\pm L}^\sigma \times P_0^\pi \Rightarrow (L+1)_{\pm L}^\pi \ (\theta\text{-components only})$$

$$L_{\pm L}^\sigma \times \bar{P}_0^\pi \Rightarrow (\overline{L+1})_{\pm L}^\pi \ (\phi\text{-components only})$$

e.g. $S_0^\sigma \times P_0^\pi \Rightarrow P_0^\pi$, $S_0^\sigma \times \bar{P}_0^\pi \Rightarrow \bar{P}_0^\pi$.

The following identities for rings (see Appendix) can be proved by analysing Stone's tensor surface harmonic equations [1-3]:

For $L > 0$: $(L+1)_{\pm L}^\pi = \bar{L}_{\mp L}^\pi$; $(L+1)_{Lc,Ls}^\pi = \bar{L}_{Ls,Lc}^\pi$

$$(\overline{L+1})_{\pm L}^\pi = L_{\mp L}^\pi; \ (\overline{L+1})_{Lc,Ls}^\pi = L_{Ls,Lc}^\pi.$$

A specific example, for a 4-membered ring, is illustrated in (*3*).

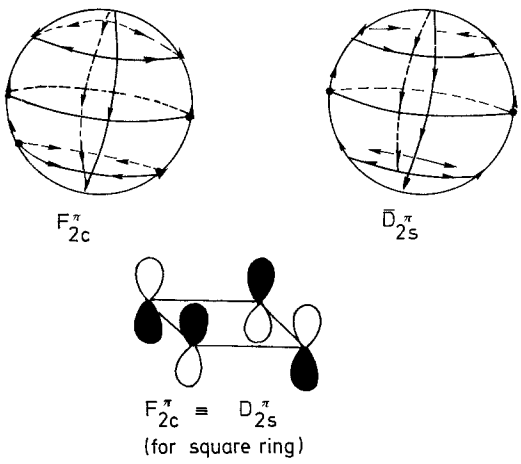

(3)

Thus, for a single ring, the spherical harmonic multiplication rules may be summarised as:

$$\text{(i)} \quad S^{\sigma}_{0} \times \begin{cases} P^{\pi}_{0} \Rightarrow P^{\pi}_{0} \text{ (purely } \theta \text{ in character; out-of plane of ring} \\ \bar{P}^{\pi}_{0} \Rightarrow \bar{P}^{\pi}_{0} \text{ } (\phi\text{; in plane of ring)} \end{cases}$$

$$\text{(ii)} \quad L^{\sigma}_{\pm L} \times \begin{cases} P^{\pi}_{0} \Rightarrow (L+1)^{\pi}_{\pm L} = \bar{L}^{\pi}_{\mp L}(\theta) \\ \bar{P}^{\pi}_{0} \Rightarrow (\overline{L+1})^{\pi}_{\pm L} = L^{\pi}_{\mp L}(\phi) \end{cases}$$

$$\text{(iii)} \quad L^{\sigma}_{Lc} \times \begin{cases} P^{\pi}_{0} \Rightarrow (L+1)^{\pi}_{Lc} = \bar{L}^{\pi}_{Ls}(\theta) \\ \bar{P}^{\pi}_{0} \Rightarrow (\overline{L+1})^{\pi}_{Lc} = L^{\pi}_{Ls}(\phi). \end{cases}$$

The interchanging of the Lc and Ls (or $+L/-L$) labels, on multiplication by $\bar{P}^{\pi}_{0}$, occurs because this function transforms as the rotation operator $\boldsymbol{R}_{z}$.

The L^{π} functions generated, using the above methodology, for rings with $n = 3-7$ vertices are listed in Table 2. The $\bar{L}^{\pi}$ functions form an identical set with matching L and M quantum numbers. The L^{π} functions exhibit approximately the same pattern as the L^{σ}'s except:

(i) P^{π}_{0} replaces S^{σ}_{0} (there is no S^{π} function, as S^{σ} has no gradient).
(ii) For $n =$ even the final term is $\mathscr{L}^{\pi}_{\mathscr{L}s}$ rather than $\mathscr{L}^{\sigma}_{\mathscr{L}c}$.

Table 2. L^{π} functions generated for planar n-gonal rings

n								
3	P^{π}_{0}	$P^{\pi}_{\pm 1}$						
4	...	...	D^{π}_{2s}					
5	...	...	$D^{\pi}_{\pm 2}$					
6	...	...	...	F^{π}_{3s}				
7	...	...	...	$F^{\pi}_{\pm 3}$				
Even n	...	...	...	...	$L^{\pi}_{\pm L}$	...	$\mathscr{L}^{\pi}_{\mathscr{L}s}$	$\mathscr{L} = n/2$
Odd n	...	...	...	...	$L^{\pi}_{\pm L}$	...	$\mathscr{L}^{\pi}_{\pm\mathscr{L}}$	$\mathscr{L} = (n-1)/2$

The values of $L_{\max}(\mathscr{L})$ and $M_{\max}$ are the same as for the L^{σ} functions.

For polyhedra consisting of 2 or more n-vertex rings lying in planes perpendicular to the principal rotation axis, similar mappings occur.

Thus, for $M=0$:

$$L_0^{\sigma}\times\begin{cases} P_0^{\pi} \Rightarrow (L+1)_0^{\pi}(\theta) \\ \bar{P}_0^{\pi} \Rightarrow (\overline{L+1})_0^{\pi}(\phi). \end{cases}$$

For $L=M=n/2$ (provided that all vertices are equivalent):

$$L_{Lc}^{\sigma}\times\begin{cases} P_0^{\pi} \Rightarrow \bar{L}_{Ls}^{\pi}(\theta) \\ \bar{P}_0^{\pi} \Rightarrow L_{Ls}^{\pi}(\phi). \end{cases}$$

For all other $L_{\pm M}^{\sigma}$ (or $L_{Mc,Ms}^{\sigma}$) pairs, multiplication by P_0^{π} and $\bar{P}_0^{\pi}$ generates tangential functions with the correct symmetry characteristics for $L_{\pm M}^{\pi}$ and $\bar{L}_{\pm M}^{\pi}$, but not the correct detailed form. In these cases π^{θ}/π^{ϕ} mixing occurs, since some (or all) of the vertices lie off the equator. It can however be seen that for any general polyhedron the presence of $L_{\pm M}^{\sigma}$ results in the occurrence of $L_{\pm M}^{\pi}$ and $\bar{L}_{\pm M}^{\pi}$. The methodology described above therefore represents a technique for enumerating the tensor surface harmonic functions for polyhedra rather than generating their precise form.

An exception to these generalisations occurs when there are 2 or more sets of eclipsed n-membered rings, with n even. In such cases the L^{σ} functions with the greatest number $(n/2)$ of vertical nodes are:

$$L_{Lc}^{\sigma}, (L+1)_{Lc}^{\sigma}, (L+2)_{Lc}^{\sigma}\cdots(L+N-1)_{Lc}^{\sigma}$$

where N is the number of eclipsed rings.

Using the above rules, multiplication of L_{Lc}^{σ} by P_0^{π} and $\bar{P}_0^{\pi}$ generates $\bar{L}_{Ls}^{\pi}$ and L_{Ls}^{π} respectively. For the functions $(L+I)_{Lc}^{\sigma}(I=1 \text{ to } N-1)$, however, the following multiplication rules apply:

$$(L+I)_{Lc}^{\sigma}\times\begin{cases} P_0^{\pi} \Rightarrow (L+I-1)_{Lc}^{\pi} \\ \bar{P}_0^{\pi} \Rightarrow (\overline{L+I-1})_{Lc}^{\pi} \end{cases}$$

because, as shown in Fig. 2, the horizontal nodes in L_{Mc}^{σ} are converted into mirror planes after multiplication by P_0^{π}.

The generalisations developed above permit the evaluation of the L^{σ} and $L^{\pi}/\bar{L}^{\pi}$ orbitals for specific classes of polyhedra without resorting to the explicit formulae of the TSH functions. The following sections are concerned with a number of classes of polyhedra which are commonly encounted in coordination and cluster chemistry.

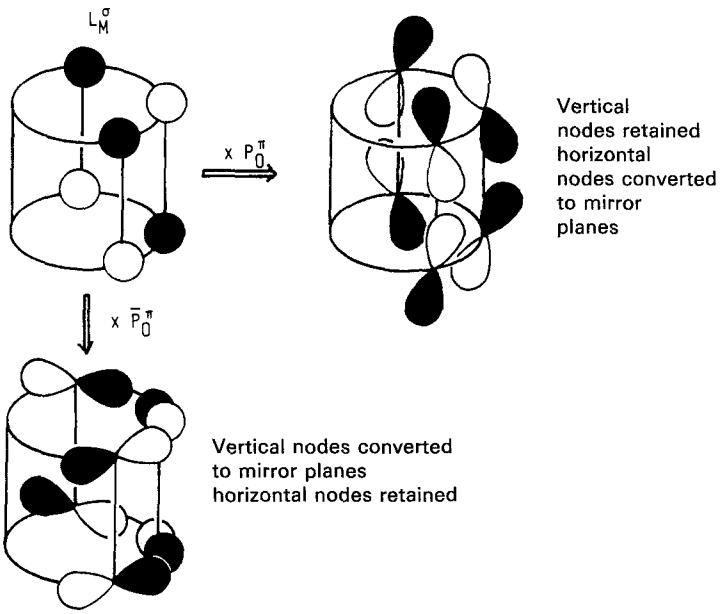

Fig. 2. The effect of multiplication by P_0^π and $\bar{P}_0^\pi$ on the horizontal and vertical nodal planes of a general L_M function

4. Prisms

Since a prism consists of a pair of eclipsed n-membered rings, linear combinations of the L^σ (or $L^\pi/\bar{L}^\pi$) functions on the two rings can be taken to generate the orbitals of the prism:

$$\Psi_{\text{prism}} = \Psi_{\text{ring 1}} \pm \Psi_{\text{ring 2}}.$$

The in-phase combinations (Ψ^+) are identical to the functions of the individual rings (i.e. the general term is $L_{\pm L}^\sigma$). The out-of-phase combinations (Ψ^-), on the other hand, possess a horizontal node in the equatorial plane. This leads to general functions of the form $(L+1)_{\pm L}^\sigma$.

The Ψ^+ and Ψ^- combinations can be generated by multiplying the spherical harmonic functions characteristic of the ring by S_0^σ and P_0^σ respectively. Multiplication by S_0^σ results in the sign and magnitude of the coefficients on the two rings being equal, while multiplication by P_0^σ (i.e. P_z) introduces a single horizontal node, thereby increasing L by one. As indicated above, for n_1 layers the L^σ functions of the single ring must be multiplied by $S_0^\sigma, P_0^\sigma, D_0^\sigma \cdots N_0^\sigma$, where $N = n_1 - 1$, such that:

$$L_{\pm L}^\sigma \times N_0^\sigma \Rightarrow (L+N)_{\pm L}^\sigma.$$

Table 3. L^{σ} functions generated for $2n$-vertex prisms

n											
3	S_0^{σ}	P_0^{σ}	$P_{\pm 1}^{\sigma}$	$D_{\pm 1}^{\sigma}$							
4	...	...	...	...	D_{2c}^{σ}	F_{2c}^{σ}					
5	...	...	...	...	$D_{\pm 2}^{\sigma}$	$F_{\pm 2}^{\sigma}$					
6	...	...	...	...	...	...	F_{3c}^{σ}	G_{3c}^{σ}			
7	...	...	...	...	...	...	$F_{\pm 3}^{\sigma}$	$G_{\pm 3}^{\sigma}$			
Even n	...	...	...	...	...	$L_{\pm(L-1)}^{\sigma}$	$L_{\pm L}^{\sigma}$	...	$(\mathscr{L}-1)_{(\mathscr{L}-1)c}^{\sigma}$	$\mathscr{L}_{(\mathscr{L}-1)c}^{\sigma}$	$\mathscr{L}=(n+2)/2$
Odd n	...	...	...	...	...	$L_{\pm(L-1)}^{\sigma}$	$L_{\pm L}^{\sigma}$	...	$(\mathscr{L}-1)_{\pm(\mathscr{L}-1)}^{\sigma}$	$\mathscr{L}_{\pm(\mathscr{L}-1)}^{\sigma}$	$\mathscr{L}=(n+1)/2$

The concept of building up structures with cylindrical topologies by stacking n-vertex rings will be discussed in more detail in a subsequent publication [23].

Table 3 lists the L^σ functions for $2n$-vertex prisms with $n = 3-7$. As indicated above, for a general value of L the functions generated are $L^\sigma_{\pm L}$ and $L^\sigma_{\pm(L-1)}$. For the L^σ functions the value of $L_{\max}$ (i.e. $\mathscr{L}$) for the $2n$-vertex prism and the n-vertex ring from which it is generated are related as follows:

$$\mathscr{L}_{\text{prism}} = \mathscr{L}_{\text{ring}} + 1$$

because the introduction of a horizontal node increases the maximum number of angular nodes ($\mathscr{L}$) by one. The L^σ functions for general $2n$-vertex prisms are listed in Table 2.

Although all of the vertices of the prism lie on the surface of a sphere, holes in the L^σ manifold are observed. This occurs because prisms do not represent an efficient way of covering a spherical surface [20].

The L^π functions generated by some prismatic geometries are listed in Table 4. Prisms are the simplest examples of the class of *non-polar polyhedra* (defined as having no atoms on the principal C_n axis [17]). As for rings, the L^π and $\bar{L}^\pi$ manifolds of non-polar polyhedral clusters are totally distinct (i.e. there are no degenerate $L^\pi/\bar{L}^\pi$ pairs) [17]. The pattern for the L^π functions is very similar to that of the L^σ functions (as for rings), with the general functions generated being $L^\pi_{\pm(L-1)}$ and $L^\pi_{\pm L}$. For odd n the L^π functions generated are the same as the L^σ (but with S^σ_0 replaced by D^π_0) and the final term is $\mathscr{L}^\pi_{\pm(\mathscr{L}-1)}$, where $\mathscr{L} = L_{\max} = M_{\max} + 1 = (n+1)/2$. In terms of the spherical harmonic multiplication rules, $S^\sigma_0 \times P^\pi_0 \Rightarrow P^\pi_0$; $P^\sigma_0 \times P^\pi_0 \Rightarrow D^\pi_0$; $L^\sigma_{\pm M} \times \bar{P}^\pi_0 \Rightarrow L^\pi_{\mp M}$.

From Table 4 it can be seen that prisms with even n have two non-degenerate highly noded π-type functions: $\mathscr{L}^\pi_{\mathscr{L}s}$ and $\mathscr{L}^\pi_{\mathscr{L}c}(\mathscr{L} = n/2)$. For the square prism ($n = 4$) these orbitals are D^π_{2s} and D^π_{2c}. [In this treatment the square prism is considered to be distorted in such a way as to possess axial (D_{4h}) rather than cubic (O_h) symmetry]. Following the arguments developed in the previous section for eclipsed-ring geometries, these L^π orbitals are derived from the L^σ functions by the following mappings (see Fig. 3):

Table 4. L^π functions generated for $2n$-vertex prisms

n										
3	P^π_0	$P^\pi_{\pm1}$	D^π_0	$D^\pi_{\pm1}$						
4	···	···	···	···	$D^\pi_{2c,2s}$					
5	···	···	···	···	$D^\pi_{\pm2}$	$F^\pi_{\pm2}$				
6	···	···	···	···	···	···	$F^\pi_{3c,3s}$			
7	···	···	···	···	···	···	$F^\pi_{\pm3}$	$G^\pi_{\pm3}$		
Even n	···	···	···	···	···	$L^\pi_{\pm(L-1)}$	$L^\pi_{\pm L}$	···	$\mathscr{L}^\pi_{\mathscr{L}c,\mathscr{L}s}$	$\mathscr{L} = n/2$
Odd n	···	···	···	···	···	$L^\pi_{\pm(L-1)}$	$L^\pi_{\pm L}$	···	$\mathscr{L}^\pi_{\pm(\mathscr{L}-1)}$	$\mathscr{L} = (n+1)/2$

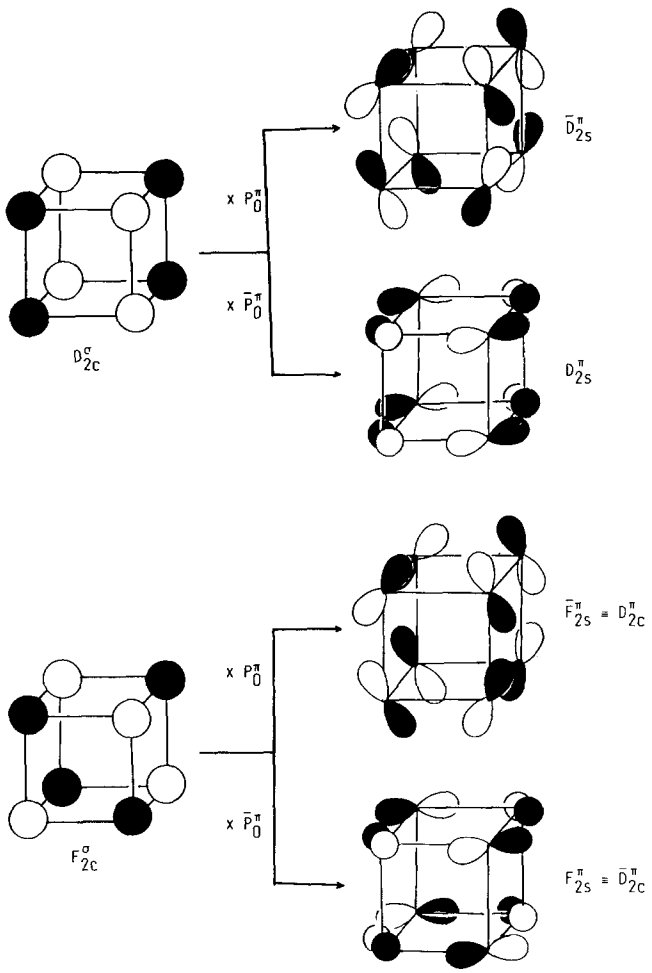

Fig. 3. Some $L^\sigma \Rightarrow L^\pi/\bar{L}^\pi$ mappings for a square prism

$$D_{2c}^\sigma \times \begin{cases} P_0^\pi \Rightarrow \bar{D}_{2s}^\pi \\ \bar{P}_0^\pi \Rightarrow D_{2s}^\pi \end{cases}$$

$$F_{2c}^\sigma \times \begin{cases} P_0^\pi \Rightarrow D_{2c}^\pi \\ \bar{P}_0^\pi \Rightarrow D_{2c}^\pi. \end{cases}$$

5. Antiprisms

Antiprismatic geometries are constructed from two n-membered rings which are staggered with respect to each other. Following the method developed above for prisms, in-phase and out-of-phase combinations are taken. Identical functions are generated by $2n$-vertex puckered rings, which have the same symmetry.

Table 5. L^σ functions generated for $2n$-vertex antiprisms

n										
2	S_0^σ	P_0^σ	$P_{\pm1}^\sigma$	(i.e. tetrahedron)						
3	...	...	...	$D_{\pm1}^\sigma$						
4	...	...	...	...	$D_{\pm2}^\sigma$					
5	...	...	...	...	...	$F_{\pm2}^\sigma$				
6	...	...	...	...	...	...	$F_{\pm3}^\sigma$			
7	...	...	...	...	...	...	...	$G_{\pm3}^\sigma$		
Even n	...	...	...	...	...	$L_{\pm(L-1)}^\sigma$	$L_{\pm L}^\sigma$	...	$\mathscr{L}_{\pm\mathscr{L}}^\sigma$	$\mathscr{L}=n/2$
Odd n	...	...	...	...	...	$L_{\pm(L-1)}^\sigma$	$L_{\pm L}^\sigma$	...	$\mathscr{L}_{\pm(\mathscr{L}-1)}^\sigma$	$\mathscr{L}=(n+1)/2$

The L^σ functions generated by some antiprismatic geometries are listed in Table 5. As for prismatic geometries, the general functions which are adopted are $L_{\pm L}^\sigma$ and $L_{\pm(L-1)}^\sigma$. For odd n, the set of L^σ functions generated by an antiprism are the same as that of the corresponding prism, with the final functions $\mathscr{L}_{\pm\mathscr{L}}^\sigma(\mathscr{L}=(n+1)/2=M_{\max}+1)$. For even n, however the final term is $\mathscr{L}_{\pm\mathscr{L}}^\sigma$ (where $\mathscr{L}=M_{\max}=n/2$). The $360°/2n$ rotation of the upper plane relative to the lower one ensures that both of the $\mathscr{L}_{\pm L}^\sigma$ functions are generated. The relationship between the $D_{2c}^\sigma/F_{2c}^\sigma$ functions of the square prism and the $D_{\pm2}^\sigma$ functions of the square antiprism are illustrated in Fig. 4.

The L^π functions generated, by the spherical harmonic multiplication rules, for some antiprismatic geometries are listed in Table 6. The L^π functions (for both even and odd n) are identical to those for the prismatic geometries.

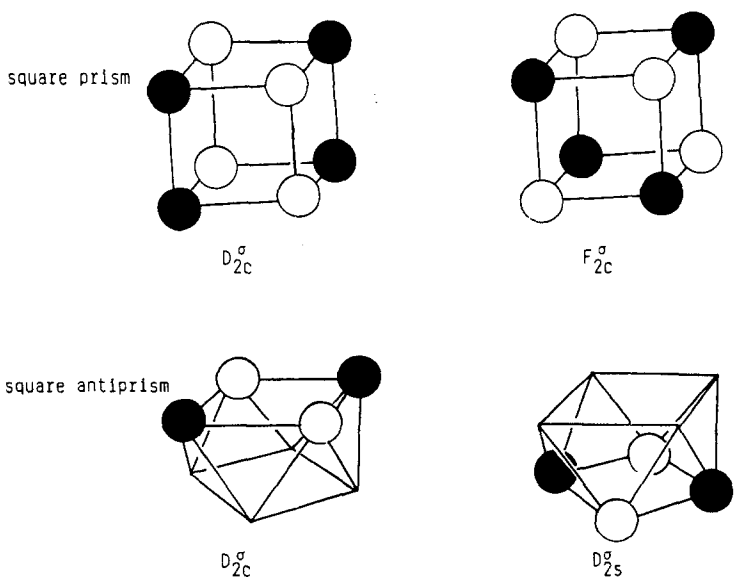

Fig. 4. Comparison of the D_{2c}^σ and F_{2c}^σ orbitals of a square prism with the $D_{2c,2s}^\sigma$ orbitals of a square antiprism

Table 6. L^{π} functions generated for $2n$-vertex antiprisms

n											
2	P_0^{π}	$P_{\pm1}^{\pi}$	D_0^{π}								
3	···	···	···	$D_{\pm1}^{\pi}$							
4	···	···	···	···	$D_{\pm2}^{\pi}$						
5	···	···	···	···	···	$F_{\pm2}^{\pi}$					
6	···	···	···	···	···	···	$F_{\pm3}^{\pi}$				
7	···	···	···	···	···	···	···	$G_{\pm3}^{\pi}$			
Even n	···	···	···	···	···	$L_{\pm(L-1)}^{\pi}$		$L_{\pm L}^{\pi}$	···	$\mathscr{L}_{\pm\mathscr{L}}^{\pi}$	$\mathscr{L}=n/2$
Odd n	···	···	···	···	···	$L_{\pm(L-1)}^{\pi}$		$L_{\pm L}^{\pi}$	···	$\mathscr{L}_{\pm(\mathscr{L}-1)}^{\pi}$	$\mathscr{L}=(n+1)/2$

6. Composite polyhedra

It has been shown above that prisms and antiprisms may be treated as two eclipsed or staggered n-membered rings, and that their L^{σ} functions (and subsequently their L^{π} functions) may be generated by taking linear combinations of the ring functions. This principle may readily be extended to a large number of polyhedral types consisting of two or more sub-sets ("orbits" [13]) of equivalent (i.e. connectivity- and symmetry-equivalent) vertices. The L^{σ} functions of these "composite polyhedra" can then be evaluated by taking linear combinations of the orbitals of the separate subsets of vertices.

6.1. Pyramids

An $(n+1)$-vertex pyramid is generated by capping an n-vertex ring, i.e. by placing a vertex on the C_n rotation axis. This vertex generates a single L^{σ} function (S_0^{σ}). This function combines with the S_0^{σ} combination of the ring,

$$\psi^{+}(S_0^{\sigma}) = S_0^{\sigma}$$
$$\psi^{-}(S_0^{\sigma}) = P_0^{\sigma}.$$

Since a pyramid is a 3-dimensional, 2-layer polyhedron (like the prisms and antiprisms), a function possessing a single horizontal node (i.e. with $M = L-1$) is allowed. The L_0^{σ} functions with $L>1$ are merely repeats of S_0 (even L) or P_0 (odd L). Thus, the L^{σ} functions of an $(n+1)$-vertex pyramid are identical to those of the parent n-membered ring, with the addition of P_0^{σ}.

The spherical harmonic multiplication rules do not apply to those polyhedra possessing vertices on the principal rotation axis. A pyramid is an example of such a polyhedron and may be classed as a "*polar polyhedron*" since there is a single (polar) vertex on the C_n axis [17]. For the L^{π} orbitals, as for the L^{σ} functions, it is necessary to take linear combinations of orbitals located on the polar and ring vertices. The polar atom possesses a single degenerated $(P^{\pi}/\bar{P}^{\pi})_{\pm1}$ pair. The combination of this pair with the $P_{\pm1}^{\pi}$ and $\bar{P}_{\pm1}^{\pi}$ orbitals of the ring (which possess the same symmetry in any C_{nv} point group) generates one $P_{\pm1}^{\pi}$ pair, one $\bar{P}_{\pm1}^{\pi}$ pair and a degenerate $(D^{\pi}/\bar{D}^{\pi})_{\pm1}$ pair. Molecular orbital calculations have shown that (*nido*) pyramidal structures do indeed possess degenerate $(D^{\pi}/\bar{D}^{\pi})_{\pm1}$ orbitals in the frontier orbital region [14, 16, 17].

Pyramids are the simplest examples of the class of polar polyhedra. It has been shown that a general polar polyhedron possesses a frontier orbital pair of degenerate $(L^{\pi}/\bar{L}^{\pi})_{\pm 1}$ orbitals, where L is equal to the number (n_1) of layers (horizontal planes) of vertices in the polyhedron (e.g. $L=2(D)$ for pyramids) [17].

6.2. Bipyramids

An $(n+2)$-vertex bipyramid is generated by placing two polar atoms on the C_n axis of an n-vertex ring. These two atoms constitute a bipole and generate S_0^{σ} and P_0^{σ} combinations. The S_0^{σ} function of the bipole combines with the S_0^{σ} function of the ring to yield $S_0^{\sigma}(\psi^+)$ and $D_0^{\sigma}(\psi^-)$. Thus, the L^{σ} functions of an $(n+2)$-vertex bipyramid are merely those of the parent n-vertex ring with the addition of P_0^{σ} and D_0^{σ}. A bipyramid is a 3-layer structure and it possesses 3 L_0^{σ} functions.

Considering the π-type functions, the bipole generates a $P_{\pm 1}^{\pi}$ and a $\bar{P}_{\pm 1}^{\pi}$ pair. Linear combinations may be taken of these functions and the $P_{\pm 1}^{\pi}$ and $\bar{P}_{\pm 1}^{\pi}$ functions of the ring:

$$\psi^+(P_{\pm 1}^{\pi}) = P_{\pm 1}^{\pi};\ \psi^-(P_{\pm 1}^{\pi}) = \bar{D}_{\pm 1}^{\pi}$$
$$\psi^+(\bar{P}_{\pm 1}^{\pi}) = \bar{P}_{\pm 1}^{\pi};\ \psi^-(P_{\pm 1}^{\pi}) = D_{\pm 1}^{\pi}.$$

Thus, the L^{π} and $\bar{L}^{\pi}$ functions generated by an $(n+2)$-vertex bipyramidal geometry are the same as those of the parent n-vertex ring, with the addition of $D_{\pm 1}^{\pi}$ and $\bar{D}_{\pm 1}^{\pi}$.

Bipyramids are the simplest examples of the class of *bipolar polyhedra* (possessing 2 vertices on the principal C_n axis) [17]. Bipolar polyhedral clusters are characterised by frontier orbital pairs of bonding $L_{\pm 1}^{\pi}$ and antibonding $\bar{L}_{\pm 1}^{\pi}$ orbitals, with $L=(n_l-1)$. The $L_{\pm 1}^{\pi}$ functions have π character (i.e. in-phase) with respect to the polar vertices if L is odd and π^* character (out-of-phase) if L is even, while the converse is true for the $\bar{L}_{\pm 1}^{\pi}$ functions [17].

7. Applications

Applications of the methodology developed above to valence and vibrational problems in inorganic chemistry are widespread and only some illustrative examples will be given below.

The composite polyhedra approach may be used to explain the spectrum of skeletal MO's in a number of classes of cluster compounds. For example, we have noted previously that N-vertex prisms and related 3-connected polyhedral clusters are characterised by $(N-2)$ approximately non-bonding parity related L^{π} and $\bar{L}^{\pi}$ orbitals [7]. This can be rationalised by generating the tangential orbitals of the prism from those of its constituent rings:

$$\psi^+(P_0^{\pi}) \Rightarrow P_0^{\pi};\qquad \psi^+(\bar{P}_0^{\pi}) \Rightarrow \bar{P}_0^{\pi}$$
$$\psi^-(P_0^{\pi}) \Rightarrow D_0^{\pi};\qquad \psi^-(\bar{P}_0^{\pi}) \Rightarrow \bar{D}_0^{\pi}$$

$$\psi^+(L^\pi_{\pm L}) \Rightarrow L^\pi_{\pm L}; \qquad \psi^+(\bar{L}^\pi_{\pm L}) \Rightarrow \bar{L}^\pi_{\pm L}$$
$$\psi^-(L^\pi_{\pm L}) \Rightarrow (L+1)^{\pi *}_{\pm L}; \qquad \psi^-(\bar{L}^\pi_{\pm L}) \Rightarrow (\overline{L+1})^{\pi *}_{\pm L}.$$

For even n:

$$\psi^+(\mathscr{L}^\pi_{\mathscr{L}s}) \Rightarrow \mathscr{L}^\pi_{\mathscr{L}s}; \qquad \psi^-(\mathscr{L}^\pi_{\mathscr{L}s}) \Rightarrow (\mathscr{L}+1)^\pi_{\mathscr{L}s} = \bar{\mathscr{L}}^{\pi *}_{\mathscr{L}c}$$
$$\psi^+(\bar{\mathscr{L}}^\pi_{\mathscr{L}s}) \Rightarrow \bar{\mathscr{L}}^\pi_{\mathscr{L}s}; \qquad \psi^-(\bar{\mathscr{L}}^\pi_{\mathscr{L}s}) \Rightarrow (\overline{\mathscr{L}+1})^\pi_{\mathscr{L}s} = \mathscr{L}^{\pi *}_{\mathscr{L}c}$$

(where the non-bonding tangential orbitals are labelled with an asterisk).

The non-bonding character of the ψ^- combinations can be rationalised in terms of their intra- and inter-ring bonding characteristics. The $\psi^-(L^\pi_{\pm L})$ combinations [i.e. $(L+1)^\pi_{\pm L}$ are bonding within each ring but antibonding between the rings. In contrast, the $\psi^-(\bar{L}^\pi_{\pm L})$ combinations [i.e. $(\overline{L+1})^\pi_{\pm L}$] are bonding between the rings. For even n, the $\psi^-(\mathscr{L}^\pi_{\mathscr{L}s})$ [i.e. $\bar{\mathscr{L}}^\pi_{\mathscr{L}c}$] function, with $\mathscr{L} = n/2$, is bonding within the rings but antibonding between them, while the converse is true for $\psi^-(\bar{\mathscr{L}}^\pi_{\mathscr{L}s})$ [i.e. $\mathscr{L}^\pi_{\mathscr{L}c}$]. The balance between intra- and inter-ring bonding/antibonding character causes all of these ψ^- combinations to be approximately non-

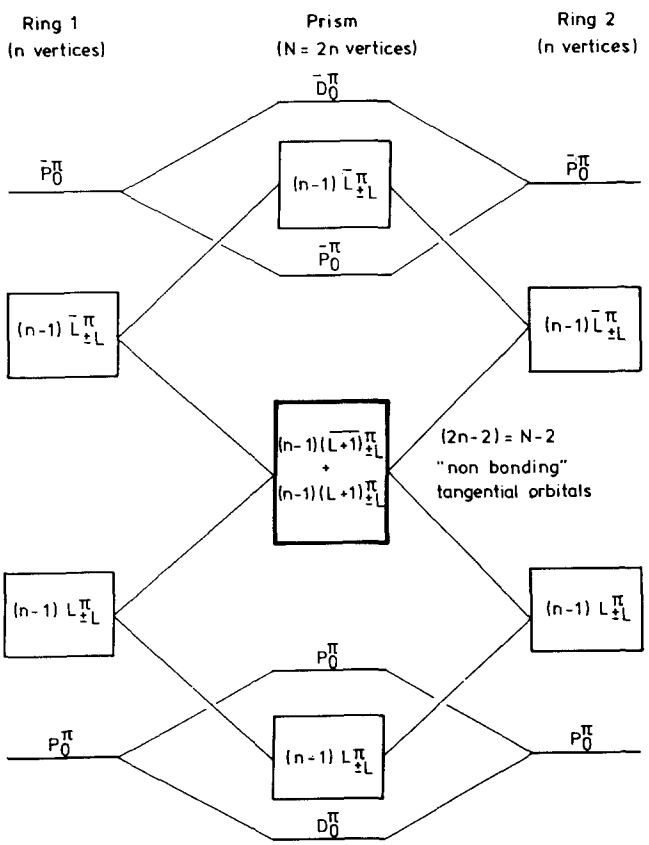

Fig. 5. Scheme depicting the spectrum of tangential MO's for prismatic clusters

Table 7. Non-bonding L^{π} and $\bar{L}^{\pi}$ orbitals for $2n$-vertex prismatic clusters

n	No. of non-bonding orbitals	L^{π}					$\bar{L}^{\pi}$					
3	4	$D^{\pi}_{\pm 1}$						$\bar{D}^{\pi}_{\pm 1}$				
4	6	$D^{\pi}_{\pm 1}$	D^{π}_{2c}					$\bar{D}^{\pi}_{\pm 1}$	$\bar{D}^{\pi}_{2c}$			
5	8	$D^{\pi}_{\pm 1}$		$F^{\pi}_{\pm 2}$				$\bar{D}^{\pi}_{\pm 1}$		$\bar{F}^{\pi}_{\pm 2}$		
6	10	$D^{\pi}_{\pm 1}$		$F^{\pi}_{\pm 2}$	F^{π}_{3c}			$\bar{D}^{\pi}_{\pm 1}$		$\bar{F}^{\pi}_{\pm 2}$	$\bar{F}^{\pi}_{3c}$	
7	12	$D^{\pi}_{\pm 1}$		$F^{\pi}_{\pm 2}$		$G^{\pi}_{\pm 3}$		$\bar{D}^{\pi}_{\pm 1}$		$\bar{F}^{\pi}_{\pm 2}$		$\bar{G}^{\pi}_{\pm 3}$
Even n	$2n-2$	$D^{\pi}_{\pm 1}$	$\cdots$	$(L+1)^{\pi}_{\pm L}$	$\cdots$	$\mathscr{L}^{\pi}_{Lc}$	$\bar{D}^{\pi}_{\pm 1}$	$\cdots$	$\overline{(L+1)}^{\pi}_{\pm L}$	$\cdots$	$\bar{\mathscr{L}}^{\pi}_{\mathscr{L}c}$	$\mathscr{L}=n/2$
Odd n	$2n-2$	$D^{\pi}_{\pm 1}$	$\cdots$	$(L+1)^{\pi}_{\pm L}$	$\cdots$	$(\mathscr{L}+1)^{\pi}_{\pm \mathscr{L}}$	$\bar{D}^{\pi}_{\pm 1}$	$\cdots$	$\overline{(L+1)}^{\pi}_{\pm L}$	$\cdots$	$\overline{(\mathscr{L}+1)}^{\pi}_{\pm \mathscr{L}}$	$\mathscr{L}=(n-1)/2$

bonding. However, the P_0^π and $\bar{P}_0^\pi$ orbitals of the ring are strongly bonding and antibonding respectively. This means that both the ψ^+ and the ψ^- combinations of P_0^π (i.e. P_0^π and D_0^π) are overall bonding, while those of $\bar{P}_0^\pi$ (i.e. $\bar{P}_0^\pi$ and $\bar{D}_0^\pi$) are both antibonding. As illustrated in Fig. 5, the total number of non-bonding tangential orbitals is [7]:

$$2(n-1) = 2n-2 = N-2.$$

The non-bonding tangential orbitals of $2n$-vertex prisms with $n = 3-7$ are listed in Table 7.

The ready access to the spherical harmonic notation is also useful for dealing with orbital pseudo-symmetry correlations. For example, the alternative ligand geometries for a five coordinate atom are square pyramidal and trigonal bipyramidal. In a molecule such as PH_5 the five occupied σ-bonding molecular orbitals can be assigned the following L^σ labels relative to their principal rotation axes:

Trigonal bipyramid	S_0^σ	P_0^σ	P_{1c}^σ	P_{1s}^σ	D_0^σ
Square pyramid	S_0^σ	P_0^σ	P_{1c}^σ	P_{1s}^σ	D_{2c}^σ.

Since completely occupied L^σ shells cannot make rearrangements orbitally forbidden, attention can be focussed exclusively on the D_0^σ and D_{2c}^σ functions (*4*). Although their nodal characteristics are different with respect to their principal axes, they are both doubly noded with respect to the 2-fold axis about which the pseudo-rotation which interconverts them takes place (i.e. they can both be denoted D_{2c}^σ and may, therefore, be correlated). A trigonal bipyramidal main group molecule, therefore, rearranges by an orbitally-allowed TBP-SP-TBP mechanism [27].

In contrast, the TBP-SP-TBP rearrangement of trigonal bipyramidal $[B_5H_5]^{2-}$ is orbitally forbidden [28] as the square pyramidal intermediate (being a polar polyhedron) possesses a degenerate $(D^\pi/\bar{D}^\pi)_{\pm 1}$ pair. Thus, as shown in Fig. 6, the TBP-SP-TBP interconversion involves the correlation of an occupied orbital (D_{1s}^π) with an unoccupied one $(\bar{D}_{1c}^\pi)$ [29].

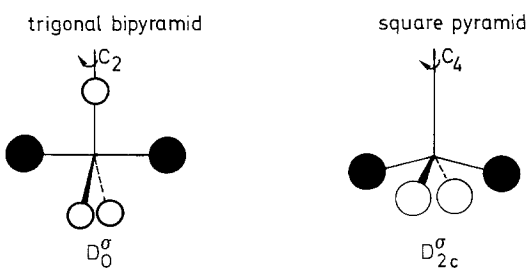

(*4*)

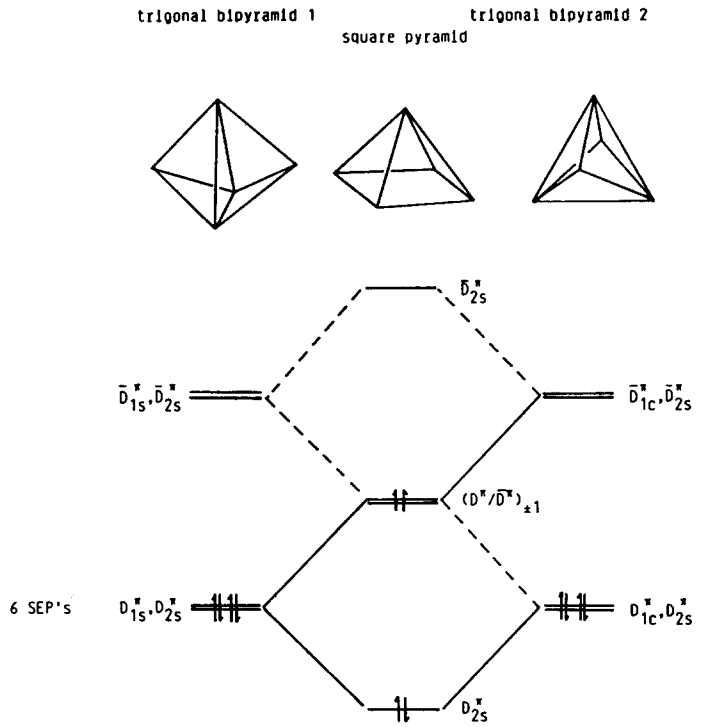

Frontier tangential orbitals for square pyramidal $[B_5H_5]^{2-}$ (6 SEP's)

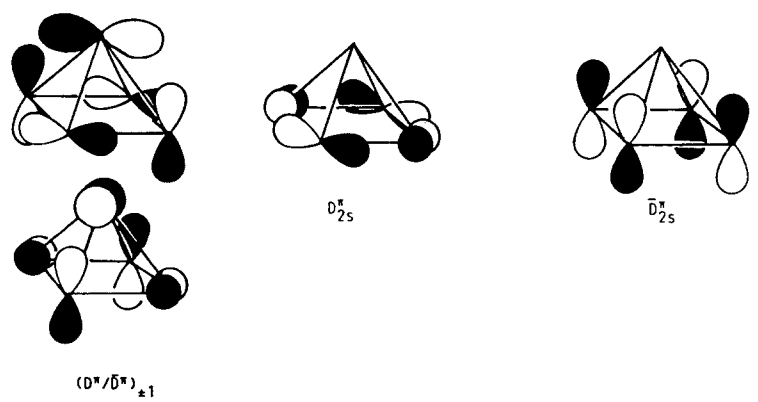

Fig. 6. Schematic representation of the forbidden nature of the TBP–SP–TBP pseudorotation for $[B_5H_5]^{2-}$

Table 8. Equivalent LCAO and LCFLO[a] functions of octahedral $[B_6H_6]^{2-}$

LCFLO function	(Skeletal bonding) LCAO function
$S^{f\sigma}(a_{1g})$	$S^{\sigma}_{sp}(a_{1g})$
$P^{f\sigma}(t_{1u})$	$(P^{\sigma}_{sp}+P^{\pi}_{p})(t_{1u})$
$D^{f\sigma}(t_{2g})$	$D^{\pi}_{p}(t_{2g})$
$F^{f\sigma}_{2c}(a_{2u})$	No Match

[a] Linear combination of face-localised orbitals

As a final example of the application of the spherical harmonic rules to problems concerning cluster bonding, an equivalent orbital [30, 31] approach has been developed which describes cluster valence orbitals in terms of spherical harmonic expansions of face- or edge-localised bonding or antibonding orbitals [32]. In the tensor surface harmonic equivalent orbital (TSHEO) approach [32] the bonding skeletal MO's of octahedral $[B_6H_6]^{2-}$ for example can be represented as linear combinations of face-localised bonding orbitals (i.e. nodeless localised orbitals located at the centers of the 8 faces of the octahedron, thereby defining a cube). Thus the skeletal bonding MO's of the octahedron are symmetry-equivalent to the L^{σ} orbitals of its face-dual polyhedron [32], the cube (these orbitals are, therefore, denoted $L^{f\sigma}$). The $L^{f\sigma}$ functions (linear combinations of localised orbitals; "LCLO's") and their LCAO equivalents are listed in Table 8. However, the $F^{f\sigma}_{2c}(a_{2u})$ combination of localised orbitals (*5*) is doubly noded with respect to each of the square faces (i.e. octahedral vertex positions) and as such cannot be generated by taking linear combinations of nodeless (σ) or singly noded (π) atomic orbitals. This leads to the conclusion that the number of allowed "face-bonding" functions is $(f-1)=7$, where f is the number of faces of the cluster polyhedron. Similar arguments, when applied to other *closo* boranes or transition metal carbonyl clusters (where the frontier orbitals are again of σ- and π-type only) reveal that all such deltahedral clusters possess $(n-5)$ "forbidden" $L^{f\sigma}$ functions, thereby enabling the $(n+1)$-SEP rule to be derived as follows:

$$\text{Number of SEP's} = \text{number of allowed } L^{f\sigma} \text{ functions} = f-(n-5)=(n+1)$$

$$(\text{since } f=2(n-2) \text{ for all deltahedra}).$$

In octahedral metal clusters with edge-bridging π-donor ligands (e.g. $[Ta_6(\mu-Cl)_{12}Cl_8]^{4-}$) the metal fragments possess δ- as well as σ- and π-type frontier orbitals and are characterised by 8, rather than 7 SEP's, since the $F^{f\sigma}_{2c}$ localised function finds a match in the $F^{\delta}_{d}(a_{2u})$ orbital (*6*) of the octahedron [22, 31].

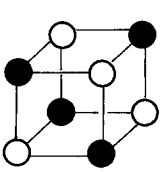

(*5*)

$F^{f\sigma}_{2c}(a_{2u})$

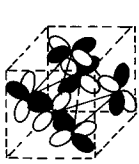

(*6*)

$F^{\delta}_{d}(a_{2u})$

8. Summary

In this paper, Stone's tensor surface harmonic theory has been used to assign pseudo-spherical symmetry labels to the valence orbitals of cluster and coordination polyhedra. Our approach has revealed the occurrence of patterns in the radial (L^σ) functions which are generated for specific classes of polyhedra. Spherical harmonic multiplication rules, analogous to Quinn's group theoretical approach, permit the evaluation of the L^π and $\bar{L}^\pi$ orbitals from the L^σ's. The $L^\pi/\bar{L}^\pi$ functions also exhibit definite patterns which reflect topological features of the polyhedra.

This simple method of evaluating the L^σ and $L^\pi/\bar{L}^\pi$ orbitals of a polyhedron can be used to simplify a wide range of bonding problems, because it retains the pseudo-spherical symmetry characteristics of the orbitals. In addition, the L^σ and $L^\pi/\bar{L}^\pi$ functions for complex polyhedra can be obtained from an *aufbau*-type procedure, whereby linear combinations of the functions of the component polyhedra are taken. This makes the qualitative aspects of the TSH methodology generally applicable and obviates the need for explicit evaluation of the L^σ, $L^\pi/\bar{L}^\pi$ etc. functions.

Appendix: Redundant L and L functions

A1. Rings

Unique functions	Redundant (i.e. equivalent) functions				
S_0^σ	D_0	G_0	$\cdots$	L_0	$L=2p;\ p=1,2,3,\ldots$
$P_{\pm1}^{\sigma,\pi}$	$F_{\pm1}$	$H_{\pm1}$	$\cdots$	$L_{\pm1}$	$L=2p+1$
$D_{\pm2}^{\sigma,\pi}$	$G_{\pm2}$	$I_{\pm2}$	$\cdots$	$L_{\pm2}$	$L=2p+2$
N_{+N}	$L_{\pm N}$				$L=2p+N.$

These redundancies may be represented by the following identity:

$$(L+2n)_{\pm L}^{\sigma,\pi} = L_{\pm L}^{\sigma,\pi} \qquad n=1,2,3,\ldots.$$

The radial functions $L_{\pm M}$ with $L+M=$ odd are noded in the plane of the ring and, therefore, are null functions. The following identity exists which relates even and odd parity tangential functions:

$$(L+1)_{\pm L}^{\pi} = \bar{L}_{\pm L}^{\pi}.$$

A2. Prisms

Unique functions	Redundant functions				
S_0^σ	D_0	G_0	$\cdots$	L_0	$L=2p$
$P_0^{\sigma,\pi}$	F_0	H_0	$\cdots$	L_0	$L=2p+1$
$P_{\pm1}^{\sigma,\pi}$	$F_{\pm1}$	$H_{\pm1}$	$\cdots$	$L_{\pm1}$	$L=2p+1$

$$\left.\begin{array}{llllll} D_{\pm 1}^{\sigma,\pi} & G_{\pm 1} & I_{\pm 1} & \cdots & L_{\pm 1} \\ D_{\pm 2}^{\sigma,\pi} & G_{\pm 2} & I_{\pm 2} & \cdots & L_{\pm 2} \end{array}\right\} L = 2p+2$$

$$\begin{array}{ll} N_{\pm(N-1)}^{\sigma,\pi} & L_{\pm(N-1)} \\ N_{\pm N}^{\sigma,\pi} & L_{\pm N} \end{array} \qquad L = 2P+N$$

These redundancies can be represented by the following identity:

$$(L+2n)_{\pm M} = L_{\pm M} \quad (\text{where } M = L \text{ or } (L-1)).$$

The following identities relate even and odd parity tangential functions:

$$(\mathscr{L}+1)^{\pi}_{\mathscr{L}s,\mathscr{L}c} = \bar{\mathscr{L}}^{\pi}_{\mathscr{L}c,\mathscr{L}s} \quad \text{for even } n\ (\mathscr{L} = n/2)$$

$$(\mathscr{L}+1)^{\pi}_{\pm\mathscr{L}} = \bar{\mathscr{L}}^{\pi}_{\mp\mathscr{L}} \quad \text{for odd } n\ (\mathscr{L} = (n+1)/2)$$

A3. Antiprisms

The redundant functions are the same as in the prismatic case, with the following identity relating even and odd parity tangential functions:

$$(\mathscr{L}+1)^{\pi}_{\pm\mathscr{L}} = \bar{\mathscr{L}}^{\pi}_{\mp\mathscr{L}} (\mathscr{L} = n/2,\ n \text{ even};\ \mathscr{L} = (n+1)/2,\ n \text{ odd}).$$

Acknowledgement. The S.E.R.C. is thanked for financial support.

References

1. Stone AJ (1980) Mol Phys 41:1339
2. Stone AJ (1981) Inorg Chem 20:563
3. Stone AJ, Alderton MJ (1982) Inorg Chem 21:2297
4. Stone AJ (1984) Polyhedron 3:1299
5. Pauling L, Wilson EB (1935) Introduction to quantum mechanics. McGraw-Hill, New York
6. Wade K (1971) J Chem Soc Chem Commun 792
7. Johnston RL, Mingos DMP (1985) J Organomet Chem 280:407
8. Johnston RL, Mingos DMP (1985) J Organomet Chem 280:419
9. Johnston RL, Mingos DMP (1987) J Chem Soc Dalton Trans 1445
10. Redmond DB, Quinn CM, McKiernan JG (1983) J Chem Soc Faraday Trans II 79:1791
11. Quinn CM, McKiernan JG, Redmond DB (1983) Inorg Chem 22:2310
12. Quinn CM, McKiernan JG, Redmond DB (1984) J Chem Ed 61:569, 572
13. Fowler PW, Quinn CM (1986) Theor Chim Acta 70:333
14. Fowler PW (1985) Polyhedron 4:2051
15. Fowler PW, Woolrich J (1986) Chem Phys Lett 127:84
16. Johnston RL, Mingos DMP (1986) Polyhedron 5:2059
17. Johnston RL, Mingos DMP (1987) J Chem Soc Dalton Trans 647
18. Mingos DMP, Johnston RL (1987) Struct Bonding Berlin, in press
19. Mingos DMP, Hawes JC (1985) J Chem Soc Chem Commun 1811
20. Mingos DMP, Hawes JC (1985) Struct Bonding Berlin 63:1
21. Mingos DMP (1987) Pure Appl Chem 59:145
22. Johnston RL, Mingos DMP (1986) Inorg Chem 25:1661
23. Johnston RL, Lin Zhenyang, Mingos DMP: to be published
24. Hoffman DK, Ruedenberg K, Verkade JG (1977) Struct Bonding Berlin 33:57

25. Verkade JG (1986) A pictorial approach to molecular bonding. Springer, New York Heidelberg Berlin
26. Brink DM, Satchler GR (1971) Angular momentum. Oxford University Press, Oxford
27. Albright TA, Burdett JK, Whangbo MH (1985) Orbital interactions in chemistry. Wiley, New York
28. Gimarc BM, Ott JJ (1986) Inorg Chem 25:83,2708; Wales DJ, Stone AJ (1987) Inorg Chem 26:3845
29. Mingos DMP, Johnston RL: Polyhedron, in press
30. Lennard-Jones JE (1949) Proc Roy Soc A 198:1, 14
31. Kettle SFA (1965) Theor Chim Acta 3:211; Kettle SFA (1966) Theor Chim Acta 4:150; Kettle SFA (1966) J Chem Soc (A) 1013; Kettle SFA, Tomlinson V (1969) J Chem Soc A 2002
32. Johnston RL, Mingos DMP: New J Chem, in press